Journal of Saudi Chemical Society (2016) xxx, xxx–xxx

King Saud University

Journal of Saudi Chemical Society

www.ksu.edu.sa
www.sciencedirect.com

ORIGINAL ARTICLE

Mercury meniscus on solid silver amalgam electrode as a sensitive electrochemical sensor for tetrachlorvinphos

Noha Al-Qasmi [a,b], A. Hameed [a,c], Amna N. Khan [b], M. Aslam [a], Iqbal M.I. Ismail [a,b], M. Tahir Soomro [a,*]

[a] *Center of Excellence in Environmental Studies, King Abdulaziz University, P.O. Box 80216, Jeddah 21589, Saudi Arabia*
[b] *Chemistry Department, Faculty of Science, King Abdulaziz University, P.O. Box 80216, Jeddah 21589, Saudi Arabia*
[c] *National Centre for Physics, Quaid-e-Azam University, Islamabad 44000, Pakistan*

Received 29 April 2016; revised 8 June 2016; accepted 19 July 2016

KEYWORDS

Organophosphate pesticide;
Tetrachlorvinphos;
Electrochemical sensor;
Mercury meniscus modified solid silver amalgam electrode;
Electrocatalytic reduction

Abstract The in-house prepared mercury meniscus modified solid silver amalgam electrode (m-AgSAE) was successfully applied for the detection of organophosphate pesticide tetrachlorvinphos in pH 7 buffer solution. The electrochemical performance of m-AgSAE for the reduction of tetrachlorvinphos was evaluated using cyclic voltammetry (CV), differential pulse voltammetry (DPV), and square wave voltammetry (SWV), respectively. The surface morphology of solid silver electrode (AgE), as-amalgamated solid silver amalgam electrode (AgSAE), and polished solid silver amalgam electrode (p-AgSAE) was examined by field emission scanning electron microscopy (FESEM). Among the applied techniques, DPV and SWV analysis showed a remarkable increase in the reduction peak current and provided a simple, fast, and sensitive method for the determination of tetrachlorvinphos. The electrochemical impedance spectroscopy (EIS) was used to correlate the electrocatalytic activity of AgSAE, p-AgSAE and m-AgSAE with their interfacial charge transport capabilities. Under the optimized experimental conditions, the DPV and SWV responses were linear over the 1–9 μM and 10–50 μM concentration ranges with a detection limit of 0.06 μM for DPV and 0.04 for SWV. The estimation of tetrachlorvinphos in the ground and waste water samples with the proposed method was in good agreement with that of the added amount. The proposed electrochemical method not only extends the application of non-toxic m-AgSAE, but also offers new possibilities for fast and sensitive analysis of tetrachlorvinphos and its structural analogs in environmental samples.

* Corresponding author.
E-mail addresses: soomro.m.tahir@gmail.com, msoomro@kau.edu.sa (M.T. Soomro).
Peer review under responsibility of King Saud University.

Production and hosting by Elsevier

http://dx.doi.org/10.1016/j.jscs.2016.07.005
1319-6103 © 2016 King Saud University. Production and hosting by Elsevier B.V.

1. Introduction

The organophosphate pesticides are the major portion (~38%) of the registered pesticides in the world (largely with U. S. Environmental Protection Agency (EPA)) and abundantly used in agriculture. It is an established fact that organophosphate pesticides are human carcinogens, and their uncontrolled usage has serious implications on health and the environment [1–4]. Due to their chemical stability, this class of pesticides is resistant to chemical and biological degradation and serves as long-term contaminants to the underground and surface water reserves. Tetrachlorvinphos, an important member of this group, has been identified as neurotoxic and caused endocrine disorders and cancer in humans and animals, particularly in children by disrupting the acetylcholinesterase enzyme [5,6]. A number of studies regarding the impaired neurological development in the children because of the exposure to the tetrachlorvinphos have been reported [7,8]. At present, the detection of organophosphate pesticides in water is regarded as a tedious task and required sophisticated instrumentation such as GC–MS and HPLC-MS [9–12]. Additionally, the extraction of the pesticide and the sample preparation for analysis is also cumbersome. Consequently, in concern over its toxicity, the direct monitoring of tetrachlorvinphos residue in the environmental samples holds great promise in practical applications.

Over the past few years, based on the inhibition or activation of the enzyme by a pesticide, enzymatic biosensors have emerged as the most promising alternative for direct determination of pesticides due to their selectivity and specificity [1,2,13–19]. The drawbacks of enzymatic methods include lack of selectivity, slow response time, and instability. More recently, direct and indirect photoelectrochemical detections of organophosphate pesticides based on the interaction of photons and the measurement of photocurrent have emerged as an innovative approach, however, the necessity of photon source and meager reproducibility is still needed to be addressed [20–23].

Since the discovery of non-toxic solid amalgam electrodes, the solid silver amalgam electrodes have been demonstrated to be very efficient electrode material specifically suited for reducible analytes [24–27]. Solid silver amalgam electrodes, due to their large negative potential window down to −2.5 V, high hydrogen overvoltage comparable with that of mercury electrode, high renewability of the electrode surface, and low detection limit, have replaced the mercury electrode in electrochemical analysis [28,29]. Among the solid silver amalgam electrodes, mercury meniscus modified solid silver amalgam electrode (m-AgSAE) presents good relative advantages: the long time stability, simple electrochemical activation, and easy renewal of mercury meniscus, which makes this electrode as a suitable choice for field monitoring. Thus, the applications of m-AgSAE for the determination of various reducible analytes such as pesticides, metals, organic, and biological compounds have been reported in the literature [30–43]. The tetrachlorvinphos contains reducible functional groups and can be electrochemically reduced in the potential window provided by the m-AgSAE. However, to the best of our knowledge, m-AgSAE coupled with voltammetric techniques for determination of tetrachlorvinphos has not been investigated at present. In the current study, differential and square wave pulse voltammetry were employed for the sensitive electrochemical detection of tetrachlorvinphos using m-AgSAE in pH 7 buffer solution.

2. Experimental

2.1. Reagents and apparatus

Stock solutions of tetrachlorvinphos (Sigma Aldrich) of concentration 1 mM were prepared by dissolution of the solid substance in ethanol, whereas the working solutions of desired concentration were freshly prepared using 0.1 M pH 7 acetate buffer. All the other reagents were of analytical grade and used as received. The morphology of solid silver electrode (AgE), solid silver amalgam electrode (AgSAE), and polished solid silver amalgam electrode (p-AgSAE) was examined with a JEOL (Tokyo, Japan) JSM 7600F field emission scanning electron microscope (FESEM). All electrochemical measurements were carried out at room temperature using a VSP multi-channel modular potentiostat/galvanostat (Bio-logic Science Instruments, France) equipped with EC-Lab software for data analysis. A voltammetric cell made up of three electrodes, a mercury meniscus modified solid silver amalgam working electrode (m-AgSAE), Ag/AgCl/saturated KCl reference electrode, and a platinum wire as an auxiliary electrode, was used. The alternating current impedance measurements at a fixed potential of −1.25 V were performed in 50 μM tetrachlorvinphos and 0.1 M pH 7 acetate buffer by sweeping the frequencies between 10 kHz and 0.1 Hz using 10 mV AC amplitude. The fitting and analysis of EIS spectra were acquired using Randle's equivalent circuit model and Z-fit (EC-Lab Software).

2.2. Preparation and activation of m-AgSAE

The solid silver amalgam electrode was prepared by the amalgamation of the solid silver electrode (disk diameter: 1.6 mm) with liquid mercury and designated as AgSAE. Prior to mercury meniscus formation, the AgSAE was polished with aqueous slurry of 0.05 μm Al_2O_3 on polyurethane pad for the removal of surface impurities and smoothing. The polished

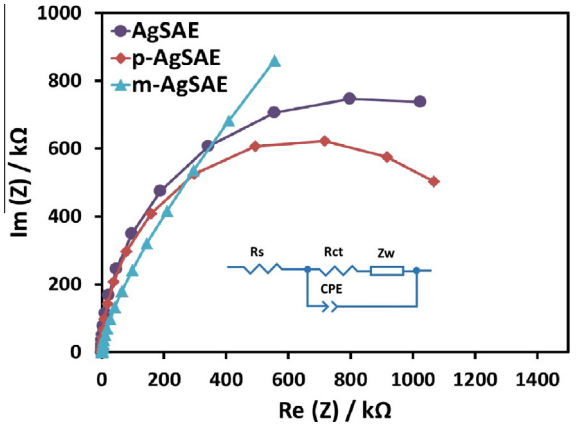

Fig. 1 Nyquist plots of the EIS spectra of AgSAE, p-AgSAE, and m-AgSAE in 50 μM tetrachlorvinphos and 0.1 M pH 7 acetate buffer at −1.25 V DC potential and 10 mV AC amplitude with frequency between 0.1 Hz and 10 kHz.

Please cite this article in press as: N. Al-Qasmi et al., Mercury meniscus on solid silver amalgam electrode as a sensitive electrochemical sensor for tetrachlorvinphos, Journal of Saudi Chemical Society (2016), http://dx.doi.org/10.1016/j.jscs.2016.07.005

Table 1 EIS fitting parameters from the equivalent circuit.

	AgSAE	p-AgSAE	m-AgSAE
Rct (kΩ)	1134	1119	18.18
Rs (Ω)	647.4	677.5	625.3
CPE (μF)	0.523	0.542	0.559

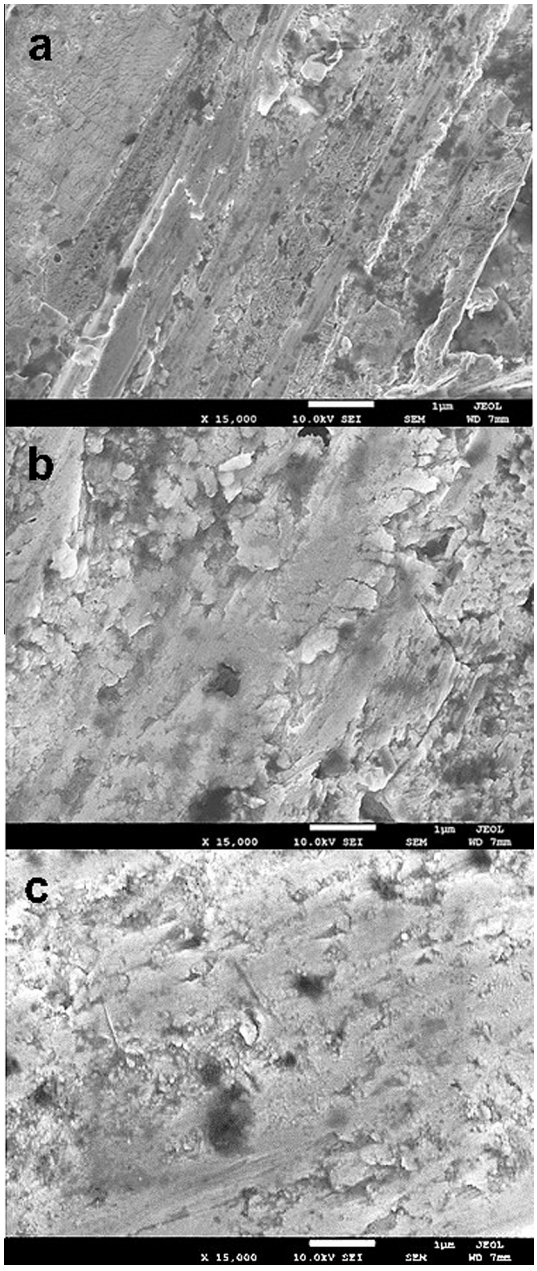

Fig. 2 FESEM images of (a) AgE, (b) as-amalgamated AgE, and (c) polished AgSAE at 15,000×.

electrode was designated as p-AgSAE. The mercury meniscus covering the electrode surface was obtained by dipping AgSAE in liquid mercury for 15 s and designated as m-AgSAE. The renewal of mercury meniscus was repeated every week. The mercury meniscus modified solid silver amalgam electrode

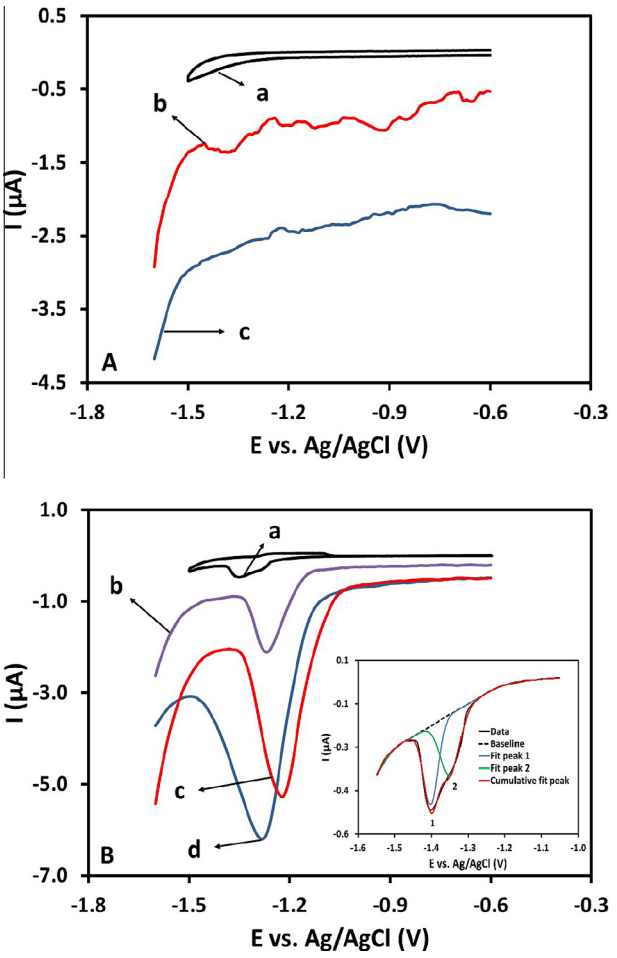

Fig. 3 CVs at 100 mV/s (a), DPVs (b and c), and SWVs (d) for m-AgSAE in (A) 0.1 M pH 7 acetate buffer, and in (B) 0.1 M pH 7 acetate buffer containing 50 μM tetrachlorvinphos. The inset shows the deconvolution and fitting of the CV response for the reduction of 50 μM tetrachlorvinphos 0.1 M pH 7 acetate buffer on m-AgSAE at 100 mV/s.

(m-AgSAE) was electrochemically activated in 0.2 M KCl solution at a negative potential of −2.2 V for 300 s, under stirring. The electrochemical activation was frequently repeated before starting the work and for every delay longer than hours to clean the electrode surface. Finally, each measurement was preceded by a short regeneration i.e. 30 s, of m-AgSAE in 0.1 M pH 7 acetate buffer at −2.2 V.

2.3. Detection of tetrachlorvinphos

10 mL of the 0.1 M pH 7 acetate buffer solution containing 50 μM tetrachlorvinphos was deoxygenated with N_2 gas for 20–25 min before the measurements. The reduction peak current proportional to the concentration of tetrachlorvinphos was detected by dipping the m-AgSAE in the voltammetric cell. The CV analysis was performed in the potential range of −0.6 and −1.5 V with a scan rate of 100 mV/s. The DPV procedure comprised an application of open circuit accumulation time of 10 s, pulse width of 100 ms, pulse height of 200 mV, and scan rate of 20 mV/s. The SWV responses were

recorded with an open circuit accumulation time of 10 s, pulse width of 70 ms, pulse height of 100 mV, and scan rate of 71.49 mV/s. The DPV and SWV scans usually range from −0.6 V to −1.6 V.

2.4. Preparation and analysis of ground and waste water samples

The ground and waste water samples (Jeddah, Saudi Arabia) were preserved at 4 °C. Prior to analysis, the particulates from water samples were removed by 0.45 μm membrane filter and transferred into volumetric flasks that were filled with ethanol. For SWV analysis, 0.5 mL of water samples was diluted with 0.1 M pH 7 acetate buffer to 10 mL.

3. Results and discussion

3.1. Alternating current impedance spectroscopy

The interfacial charge transfer resistance of the three electrodes i.e. AgSAE, p-AgSAE, and m-AgSAE in the presence of 50 μM tetrachlorvinphos in 0.1 M pH 7 acetate buffer was probed over a frequency range of 10 kHz down to 0.1 Hz at −1.25 V by alternating current impedance spectroscopy (EIS). The comparison of the Nyquist plots of the EIS spectra of AgSAE, p-AgSAE, and m-AgSAE is presented in Fig. 1 whereas the Randle's equivalent circuit model presented in the inset of Fig. 1 was used for fitting of the EIS spectra. In the Randel's circuit, the charge transfer resistance (Rct) of the electrode–electrolyte interface equal to the diameter of the semicircle was obtained from the middle-frequency intercept whereas the intercept at higher frequency was attributed to the electrolyte and the contact resistance (Rs). The CPE represented the interfacial capacity of the electrode–electrolyte interface and Zw was the Warburg impedance described by the mass transfer of the analyte to the electrode surface [44–48]. It was observed that there was not much difference in the impedance of AgSAE and p-AgSAE, the impedance of m-AgSAE was far less than that of AgSAE and p-AgSAE, and appeared almost as a linear line, which indicated excellent conductivity and seamless electron transport on m-AgSAE-electrolyte interface. This effect, the significant decrease in the kinetic barrier for the charge transfer, is likely due to the reduction of oxide (mercury or silver) layers and desorption of adsorbed species. The evaluated EIS parameters are summarized in Table 1. The results showed small differences in CPE which implied that the electroactive area of all the three

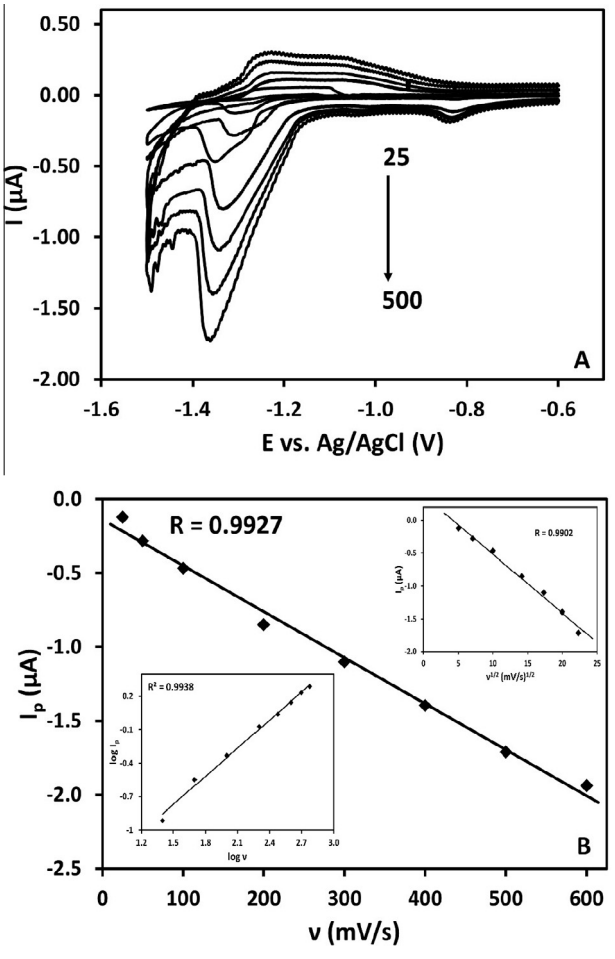

Fig. 4 (A) CVs of tetrachlorvinphos on m-AgSAE with scan rates of 25, 50, 100, 200, 300, 400, and 500 mV/s in 0.1 M pH 7 acetate buffer. (B) Plot of reduction peak current versus scan rate, the insets show the plot of reduction peak current versus the square root of scan rate and the plot between logarithm of the peak current and the logarithm of scan rate.

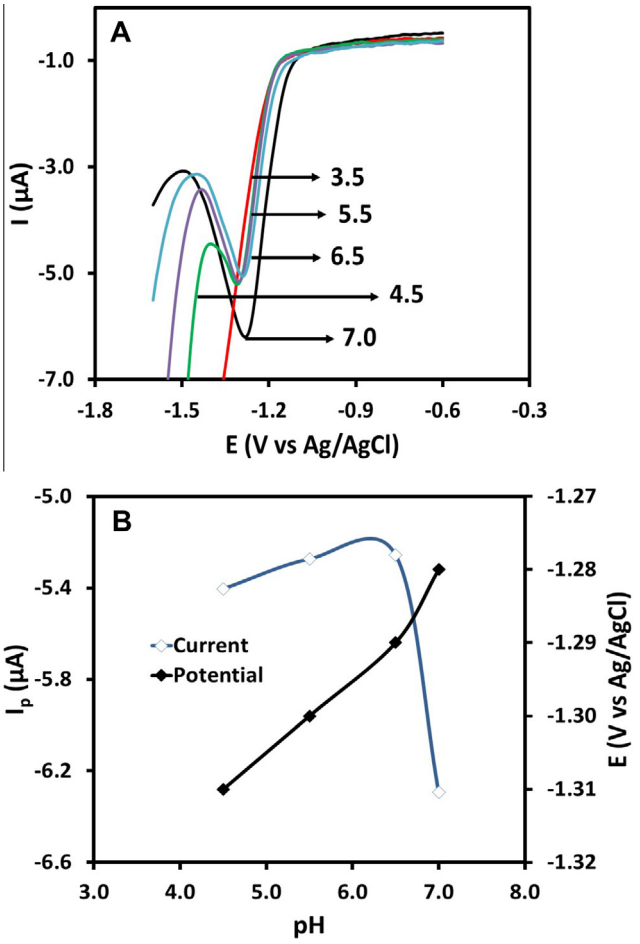

Fig. 5 (A) Effect of pH on the SWV responses of m-AgSAE in 50 μM tetrachlorvinphos. (B) The variation in the reduction peak potential and the reduction peak current with pH.

electrodes was the same, however, because of the lowest charge transfer resistance, the m-AgSAE had higher conductivity, good electrocatalytic activity, and better analytical performance for sensitive detection of tetrachlorvinphos.

3.2. Scanning electron microscopy

The FESEM images of solid silver electrode (AgE), as-amalgamated AgE, and polished AgSAE at 15,000× are compared in Fig. 2(a)–(c). Compared with AgE, the image of as-amalgamated electrode revealed the layer-by-layer deposition of the mercury on solid silver electrode with significant inhomogeneity and roughness at the surface, whereas due to the polishing, the excessive Hg layer is removed from the electrode surface thus imparting a uniform and regular pattern. Afterward, the solid silver electrode was immersed into a small volume of liquid mercury. This covering of the surface of the solid silver amalgam electrode with mercury meniscus may enable m-AgSAE to be a good electrode material for electrochemical reduction of tetrachlorvinphos.

3.3. Electrocatalytic reduction of tetrachlorvinphos on m-AgSAE

The CV, DPV, and SWV behavior of m-AgSAE in 0.1 M pH 7 acetate buffer is compared in Fig. 3A. In the absence of tetrachlorvinphos, the CV (curve a), DPV (curve b), and SWV (curve c) responses of m-AgSAE revealed no redox peak that indicated the transparency of reduction and oxidation reaction of acetate buffer in the selected potential window. A larger background current in the DPV (curve b) and SWV (curve c) measurements, compared to CV (curve a), was attributed to the high surface activity of m-AgSAE due to nearly zero charging current.

The CV (curve a), DPV (curve b & c), and SWV (curve d) current signals of 50 μM tetrachlorvinphos on m-AgSAE in 0.1 M pH 7 acetate buffer are presented in Fig. 3B. In the CV (curve a), there was a well-defined peak distinctly appeared at ~−1.35 V caused by the two consecutive one-electron reduction of C═C bond and an ill-defined shoulder peak spotted at ~−1.29 V attributing to the two consecutive one-electron reduction of P═O bond of phosphate diester group. The two reduction peaks that appeared nearly at the same potential were irreversible and coalesced to an extended reduction peak at a scan rate of 200 mV/s or higher. As expected, DPV (curve b & c) displayed a well-resolved and enhanced peak for the reduction of tetrachlorvinphos (curve b) compared to that with CV (curve a). The intensity was further enhanced upon increasing the pulse amplitude (curve c) that depicted the better catalytic and interfacial adsorptive ability of m-AgSAE coupled with DPV for tetrachlorvinphos. As DPV is a low amplitude differential technique, naturally, the higher peak current is achieved at larger pulse amplitude. In SWV (curve d) analysis, the reduction peak current for tetrachlorvinphos greatly increased as compared to those other two techniques. Under identical experimental conditions, this reduction peak current with SWV (curve d) was 7 times of that with CV (curve a), and 3–4 times of that with DPV (curve b) that attributed to the larger amplitude and very fast rate of square wave pulse application, which facilitated the highly sensitive determination of tetrachlorvinphos on m-AgSAE. In addition, because of an inherent sensitivity of DPV and SWV, the observed reduction peak potential of tetrachlorvinphos was more positive than that with CV, therefore leading to greater affinity for tetrachlorvinphos reduction. These

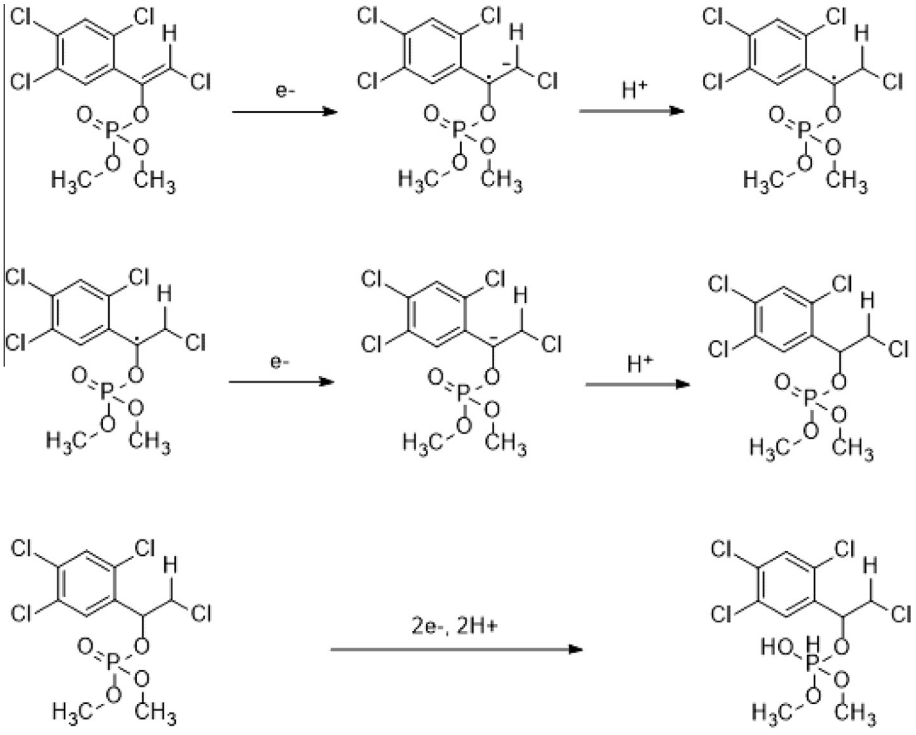

Scheme 1 Reduction mechanism of tetrachlorvinphos on m-AgSAE.

Please cite this article in press as: N. Al-Qasmi et al., Mercury meniscus on solid silver amalgam electrode as a sensitive electrochemical sensor for tetrachlorvinphos, Journal of Saudi Chemical Society (2016), http://dx.doi.org/10.1016/j.jscs.2016.07.005

findings suggested the suitability of DPV and SWV for the direct electrochemical determination of tetrachlorvinphos.

The electrochemical reduction of unsaturated C═C bond is a well-known process that occurs at more negative potentials whereas the reduction of P═O bond occurs at potentials positive than that of reduction potential of C═C bond [49–51]. It was perceived that the application of deconvolution on the CV response of the electrochemical reduction of tetrachlorvinphos (curve a, Fig. 3B), the overlapping unresolved reduction peaks can be differentiated. The deconvolution and fitting of the CV response for the reduction of tetrachlorvinphos at the scan rate of 100 mV/s is presented in the inset of Fig. 3B where the reduction peak potentials and currents associated with the reduction of C═C (peak 1) and P═O (peak 2) bonds are clearly recognizable.

3.4. Effect of scan rate

The effect of varying scan rates i.e. in the range of 25–500 mV/s on the CVs of m-AgSAE in 50 μM tetrachlorvinphos and 0.1 M pH 7 acetate buffer is presented in Fig. 4A. The intensity of the reduction peak current progressively increased upon the increase of the scan rate with a shift of reduction peak potential toward the negative potentials indicating that the reduction of tetrachlorvinphos on m-AgSAE is an irreversible reaction. In this case, the rate-determining step is the rate of electron transfer from the electrode to tetrachlorvinphos. The variation in the reduction peak current as a function of the applied scan rate is plotted in Fig. 4B, in which a straight line I_p (μA) = −0.137–0.0031 υ (mV/s) (R^2 = 0.9927) was observed. The 3.1 μA s V^{-1} slope suggesting that the reduction of tetrachlorvinphos was strongly affected by the adsorption of tetrachlorvinphos on m-AgSAE. The plot of peak current versus the square root of the scan rate presented in the inset of Fig. 4B was also found linear, which is explained by the diffusion of tetrachlorvinphos from solution to m-AgSAE. Moreover, a linear relationship between the logarithm of the peak current and the logarithm of scan rate (inset of Fig. 4B) with a slope of 0.82 (R^2 = 0.9938) was observed. Since the slope value falls between the theoretical values for diffusion and adsorption controlled processes, therefore the reduction of tetrachlorvinphos on m-AgSAE is influenced by both diffusion and adsorption mechanisms, respectively.

3.5. pH effect and reduction mechanism of tetrachlorvinphos on m-AgSAE

The effect of pH upon SWV responses for the reduction of 50 μM tetrachlorvinphos in 0.1 M pH 7 acetate buffer on m-AgSAE is presented in Fig. 5A, whereas the reduction peak potential and the reduction peak current as a function of pH are plotted in Fig. 5B. As can be seen, with the increase of the pH the reduction peak potential of tetrachlorvinphos shifted in the positive direction indicating that protons did not participate in the rate-determining step of the reduction of tetrachlorvinphos. The plot of peak potential versus pH i.e. *Ep* (V) = −1.363 + 0.0 115 pH (R = 0.9797), revealed a slope of 11 mV that further supported the independent electron transfer without associated proton involvement in the rate-determining step. The reduction peak current of tetrachlorvinphos on m-AgSAE decreased slightly in the pH range of 4.0–6.5 whereas a sharp increase was observed afterward. The lower peak current in acidic solution is probably due to the dominant role of adsorption, which may be conducive to the passivation of the electrode surface, therefore, the reproducibility of the reduction peak current was rather poor in pH lower than 7. The stable current signals with better reproducibility were observed in pH 7 acetate buffer.

Analyzed from the above results it is suggested that the unprotonated form of tetrachlorvinphos is adsorbed and reduced at the catalytic active site of m-AgSAE by two consecutive one-electron transfers, with an initial formation of radical anion, proton abstraction from the solvent, subsequent reduction to an anion followed by rapid protonation in aqueous solution resulting the C–C saturated bond. The mechanism for reduction of tetrachlorvinphos is presented in Scheme 1.

Elaborating further, it is proposed that in the tetrachlorvinphos molecule, the C═C bond is not the only electroactive site, but also the P═O bond of phosphate di-ester group is irreversibly reduced in two consecutive one-electron process. Additionally, the unresolved reduction peak of the P═O bond is scan rate dependent and gradually overlaps with the main

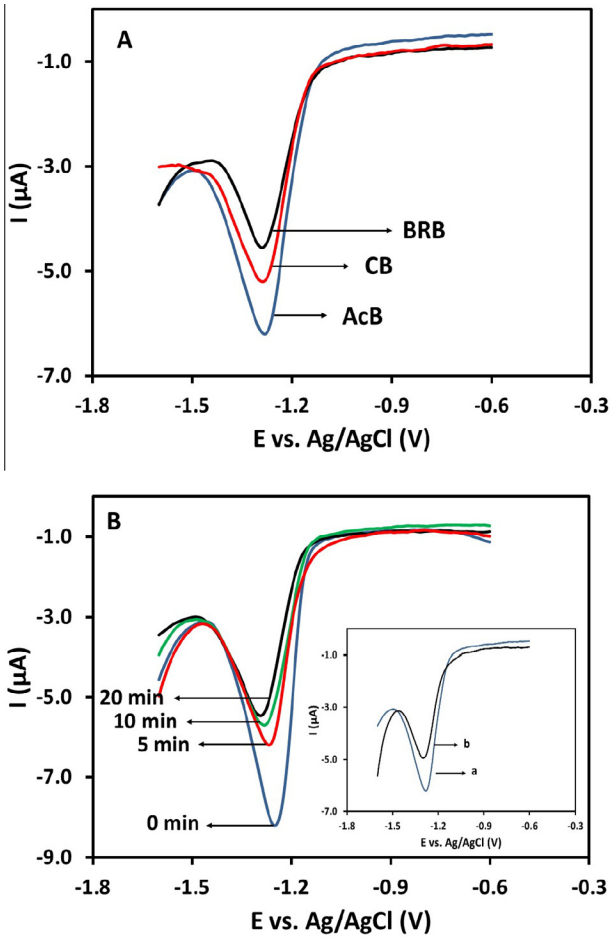

Fig. 6 (A) SWVs of m-AgSAE in 0.1 M pH 7 acetate buffer, 0.1 M pH 7 citrate buffer, and 0.1 M pH 7 Britton-Robinson buffer. (B) Variation in the reduction peak with the decreasing concentration of dissolved oxygen. The inset shows the variation in peak current under stirring.

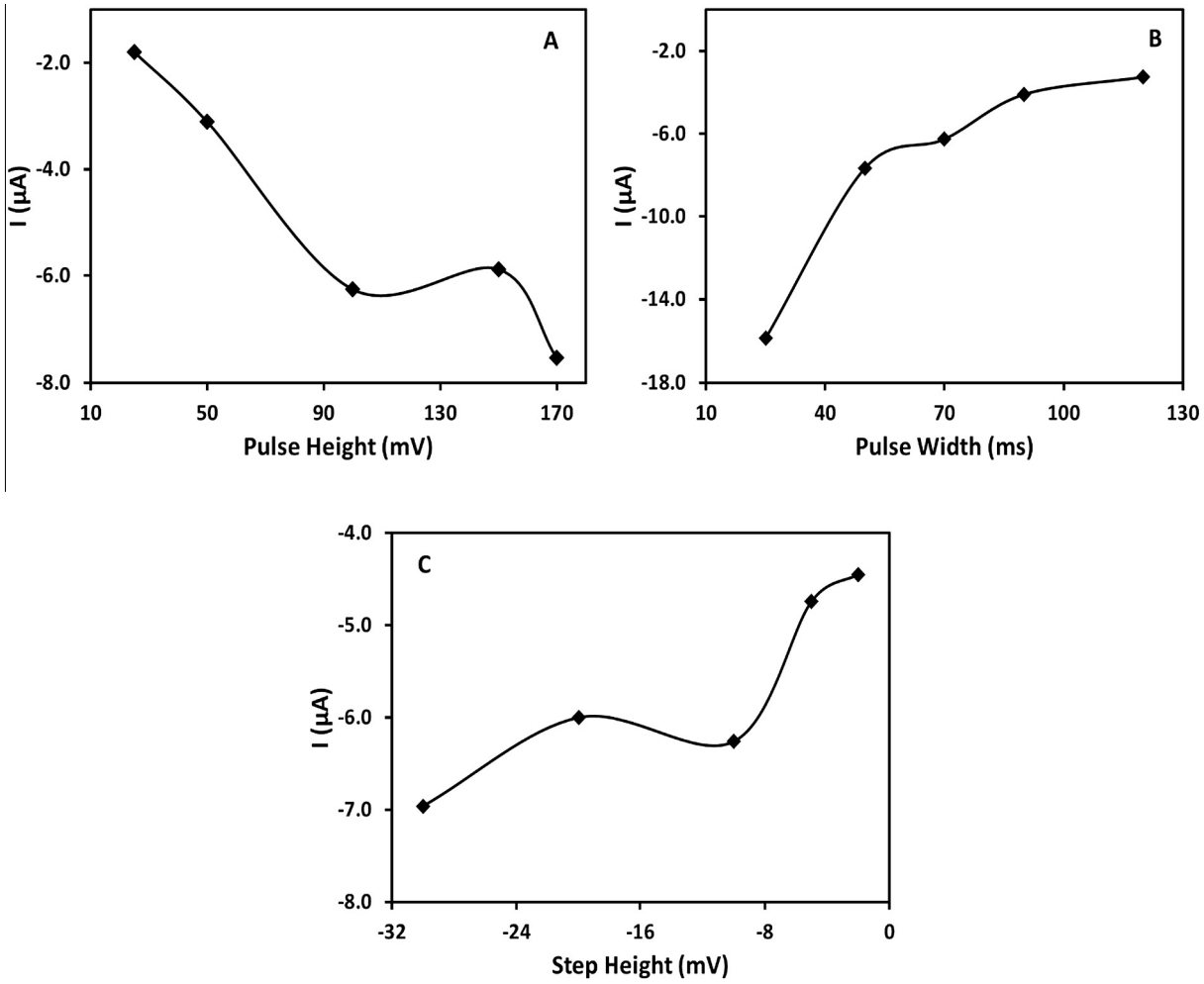

Fig. 7 Effect of the SWV parameters on the reduction peak current. The peak height and peak area depends on (A) pulse amplitude, (B) pulse width, and (C) step potential.

reduction peak (C═C) with the increasing scan rate. Probably, in the tetrachlorvinphos molecule the electron cloud density at C═C bond due to the presence of electron withdrawing groups is slightly distorted compared to P═O bond that results in the pair of unresolved reduction peaks. Furthermore, the significantly high steric hindrance and mesomeric effect makes P═O bond less prone to undergo reduction reactions that may be the probable reason for the disappearance of P═O reduction peak at higher scan rates. As nil participation of protons in the rate-determining step has been established in the reduction reaction of tetrachlorvinphos on m-AgSAE, a single well-defined DPV or SWV peak is likely to be attributed to the two electron transfer in two steps to C═C bond. Since the peak current showed a maxima in pH 7 acetate buffer with better developed peak shape, therefore all the subsequent measurements were carried out in neutral solution.

3.6. Optimal conditions for tetrachlorvinphos determination

Fig. 6A shows the comparison of SWV curves of m-AgSAE for the reduction of 50 µM tetrachlorvinphos in 0.1 M pH 7 acetate buffer (AcB), 0.1 M pH 7 citrate buffer (CB), and 0.1 M pH 7 Britton-Robinson buffer (BRB), respectively. Compared to the other two buffer solutions, the well-shaped reduction peak with higher current without the shifting in the peak potential was observed in acetate buffer for tetrachlorvinphos. Therefore, all the subsequent studies were performed in acetate buffer. The expected interference from the dissolved oxygen in the determination of tetrachlorvinphos was evaluated by purging the tetrachlorvinphos solution with N_2 gas. The optimum purging time was investigated by purging the solution for various intervals of time. The variations in the reduction peak current as a function of nitrogen purging time are presented in Fig. 6B. The reduction peak current decreased dramatically with decreasing concentration of dissolved oxygen. The electrogenerated oxygen species such as superoxide can act as a nucleophile as well as an electron donor that might be responsible for the increase of reduction peak current of tetrachlorvinphos therefore, for each measurement the solution in the voltammetric cell was deoxygenated with nitrogen sparging lasting for about 25 min. The adsorption behavior of tetrachlorvinphos and its reduction products was estimated by controlling the stirring of the solution as it could affect the diffusion of the tetrachlorvinphos molecules from the bulk solution to the electrode surface. As shown in the inset of Fig. 6B, the peak current in curve b (without

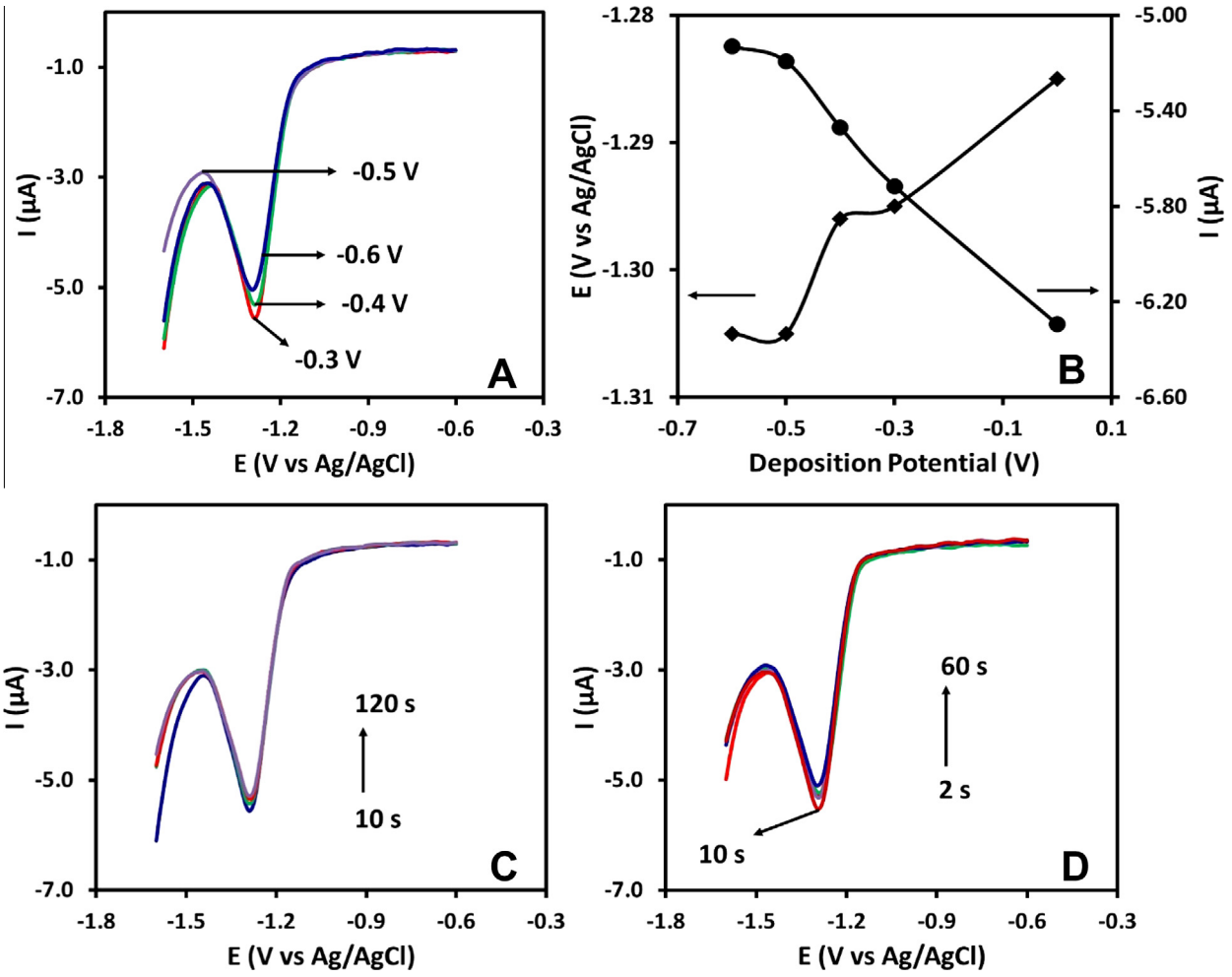

Fig. 8 (A) SWVs of m-AgSAE in 50 μM tetrachlorvinphos and 0.1 M pH 7 acetate buffer with different deposition potentials. (B) Variation in the peak current and the peak potential with changing deposition potential. SWVs with different (C) deposition and (D) equilibrium time.

Table 2 Estimated tolerance level of interfering species in the determination of tetrachlorvinphos.

Interferent	Tolerance (μM)	RSD (%)
Glucose, urea, ascorbic acid, citric acid, paracetamol	5000	2.1
Zn^{2+} Cu^{2+} Fe^{3+}, Fe^{2+},	2500	4.1
K^+, Na^+, PO_4^{2-}, SO_4^{2-}, Ca^{2+}, NH_4^+, NO_3^-	2500	2.1
Tetradifon, dichlofenthion	20	5.5
3-chlorophenol, 2,4-dinitrophenol	10	5.8

stirring) is significantly lower than that in curve a (stirring), which is due to the fact that tetrachlorvinphos molecules excessively adsorbed/diffused at the electrode surface and block the electron transfer when there is no stirring. This also implies that the reduction of tetrachlorvinphos is a diffusion controlled process and strongly influenced by the adsorption. The adsorption of the reduction products of tetrachlorvinphos on m-AgSAE was estimated by using the same electrode in 0.1 M pH 7 acetate buffer without tetrachlorvinphos after rinsing. The adsorption of the reduction products was confirmed by the appearance of a quasi-reversible redox pair of low intensity at ~−0.96 V, which indicated that the tetrachlorvinphos reduction products were adsorbed on the surface of m-AgSAE. The adsorbed reduction products were removed from the surface of the electrode by electrochemical activation and regeneration of m-AgSAE.

As shown in Fig. 7A, the reduction peak current increased with the increasing pulse amplitude from 30 mV to 100 mV followed by a decrease at 150 mV. The further increase in pulse amplitude resulted in the increased peak current. It could be explained that with the increase of the pulse amplitude the rate of tetrachlorvinphos reduction was increased. The effect of pulse width on the peak current (Fig. 7B) in the range of 20–130 ms revealed a decrease in the peak current upon increasing the pulse width, whereas with the increasing of potential step increment (Fig. 7C) the peak current increased

Table 3 Comparison of detection methods for tetrachlorvinphos.

Methods	LR	R	LOD	Stability	Recovery	Ref
SWV	10–50 μM	0.9906	0.61 μM	95%	93.1–106.2%	Present Study
	1−9 μM	0.9931	0.04 μM	(14 days)		
DPV	10–50 μM	0.9942	0.48 μM	95%	–	Present Study
	1–9 μM	0.9936	0.06 μM	(14 days)		
HPLC-MS/MS	6.25–200 μg/kg	0.9983	0.22 μg/kg	–	86–106%	[6]
	6.25–500 μg/kg	0.9968	0.25 μg/kg		93–100%	
	6.25–100 μg/kg	0.9980	0.38 μg/kg		94–102%	
DLLME-HPLC	5–200 μg/L	0.9999	0.98 μg/L	–	97–117%	[9]
SBSE-GC–MS/MS	10–500 μg/kg	–	< 1 μg/kg	–	–	[11]
Optical biosensor	4–80 μM	0.995	1 μM	15 days	95%	[14]
	0.4–40 μM	0.992	0.15 μM			

LR = linear range, LOD = limit of detection, SWV = square wave voltammetry, DPV = differential pulse voltammetry, DLLME = dispersive liquid–liquid microextraction,

rapidly at −10 mV and slightly decreased afterward. This means that, the greater reduction peak current for tetrachlorvinphos was achieved with shorter pulses and smaller step duration. Thus, the study exposed the dependence of the sensitive detection of tetrachlorvinphos on the optimal combination of instrumental parameters: pulse amplitude of 100 mV, pulse width of 70 ms, step potential of −10 mV, and scan rate of 71.4 mV/s.

The adsorptive accumulation of tetrachlorvinphos under deposition potential over the range of −300 to −600 mV (Fig. 8A) has negative effects on the reduction peak current. The accumulation of the tetrachlorvinphos resulted in the decrease in the reduction peak current due to the formation of passivating film and prevented the tetrachlorvinphos from reaching to the surface of m-AgSAE. Although, the peak potential is shifted toward more negative potentials with the change in the deposition potential (Fig. 8B) however, the time effect of deposition potential of −0.3 V showed a negligible variation in the reduction peak current (Fig. 8C). The dependence of the reduction peak current at the equilibrium time (standby potential), varied from 2 to 60 s (Fig. 8D) under open circuit potential conditions, revealed that an equilibrium time of 10 s was favorable for the determination of tetrachlorvinphos.

3.7. Interferences

Under the optimal conditions, the interfering effects of the presence of various substances such as chlorophenols, nitrophenols, tetradifon, and dichlofenthion on the sensitive detection of tetrachlorvinphos were evaluated. The relative standard deviation of three measurements of 50 μM tetrachlorvinphos in the presence of various possible interferents is presented in Table 2 considering > ±5% RSD as a deviation in the electrochemical response of tetrachlorvinphos. Interestingly, a 100-fold concentration ratio of glucose, urea, ascorbic acid, citric acid, paracetamol; 50-fold concentration ratio of Zn^{2+}, Cu^{2+}, Fe^{3+}, Fe^{2+}; and a 50-fold concentration ratio of K^{+}, Na^{+}, PO_4^{2-}, SO_4^{2-}, Ca^{2+}, NH^{4+}, NO^{3-} had an ignorable influence on the determination of tetrachlorvinphos. However, 20 μM tetradifon, 20 μM dichlofenthion, 10 μM 3-chlorophenol and 10 μM 2,4-dinitrophenol did interfere with the tetrachlorvinphos signal due to the electroactive group that can be reduced near the reduction potential of tetrachlorvinphos (Fig. S1, Supplementary details).

3.8. Electrode reproducibility and stability

The reproducibility and stability of m-AgSAE were ensured for long-term analysis. When CV used to detect the tetrachlorvinphos twenty times in parallel (Fig. S2A, Supplementary details) on m-AgSAE, the variation coefficient was 1.1%. The peak current for 50 μM tetrachlorvinphos retained 99% of its initial response with no shift in the peak potential. Furthermore, the day-to-day variation in the repeatability coefficient for multi-CV scans was within 1.7%, showing an excellent reproducibility of the electrode. The stability of the electrode was evaluated in two weeks duration (Fig. S2B, Supplementary details). The stability variation coefficient estimated after two weeks for m-AgSAE was below 5%, indicating the high stability of the electrode.

3.9. Analytical performance of m-AgSAE

SWV and DPV analysis of tetrachlorvinphos showed a greatly improved reduction peak under optimum experimental conditions. Calibration plots based on the reduction peak current proportional to the concentration of tetrachlorvinphos were linear. Fig. 9A shows the SWV curves of different concentrations of tetrachlorvinphos and the corresponding calibration plot in the inset of Fig. 9A. Two linear relationships between the reduction peak current and the concentration of tetrachlorvinphos covering the concentration ranges from 1 to 9 μM and 10 to 50 μM, and their corresponding linear equations were I (μA) = −3.223 − 0.0561 C (μM) (R = 0.9906) and I (μA) = −2.3608 − 0.1512 C (μM) (R = 0.9972). The detection limit was reached 0.04 μM [3.3 (standard error in blank/slope)] at a signal-to-noise ratio of 3. The DPV curves of different concentrations of tetrachlorvinphos and the corresponding calibration plot are presented in Fig. 9B. The linear concentration ranges from 1 to 9 μM and 10 to 50 μM with a detection limit (S/N = 3) of 0.06 μM were obtained where the linear equations were I (μA) = −2.37 − 0.057 C (μM) (R = 0.9942) and I (μA) = −1.78 − 0.1383 C (μM) (R = 0.9936), respectively. The results obtained from SWV and DPV analysis were in accordance, however, the SWV is more promising for quantitative determination of tetrachlorvinphos. Moreover, the rapid increase in the reduction peak current at low concentrations and then slow increase at higher concentration is observable from Fig. 9A or B, which is due to

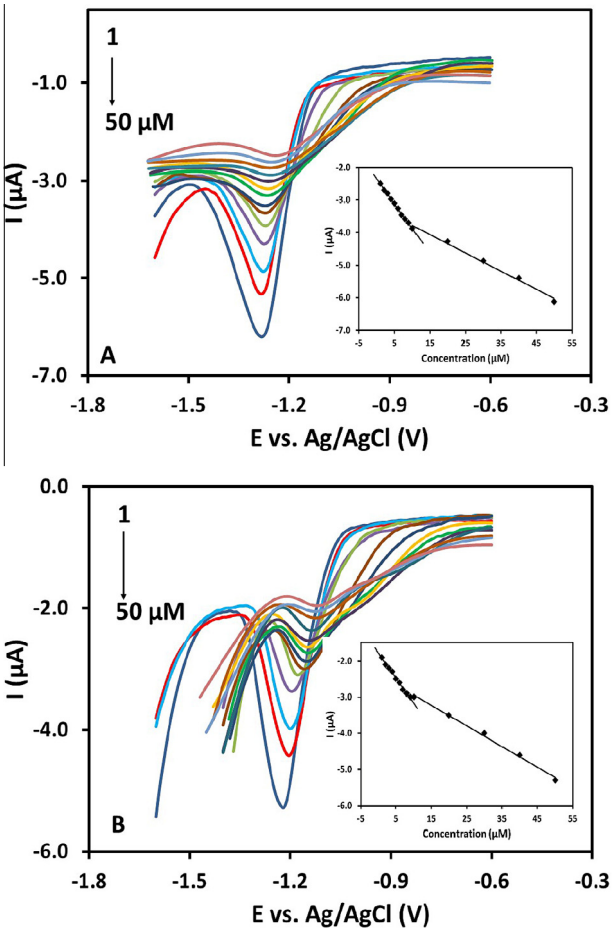

Fig. 9 (A) SWV and (B) DPV curves for different concentration of tetrachlorvinphos in 0.1 M pH 7 acetate buffer and their corresponding calibration plots in the inset.

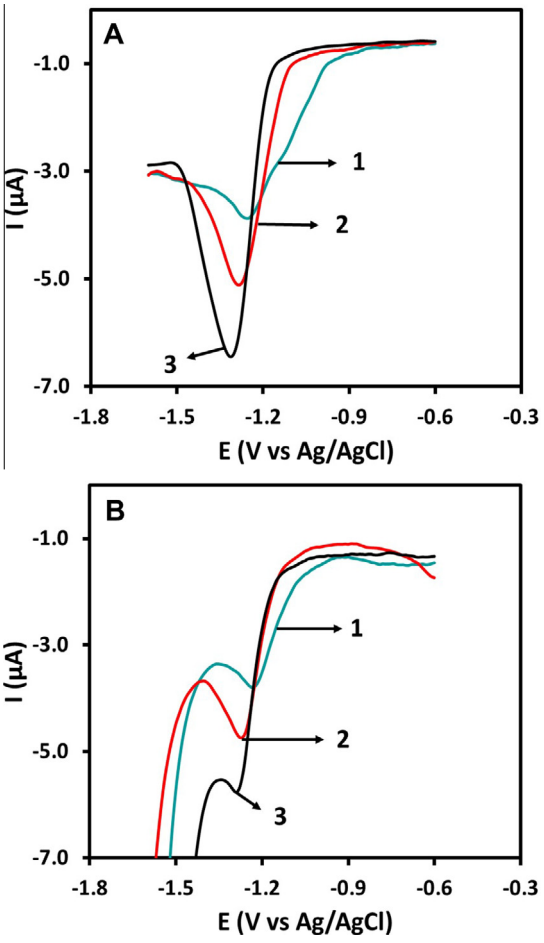

Fig. 10 SWVs of m-AgSAE in (A) the ground and (B) waste water samples.

the adsorption of tetrachlorvinphos reduction products. The brief comparison of the results with other methods was carried out (Table 3) and it was found that the detection limit for tetrachlorvinphos was inferior to that of HPLC-MS, and GC–MS but well below the maximum limit set by U.S. EPA [52]. Thus, different from the instrumental methods the proposed methods based on m-AgSAE with short detection time and low detection limit are more feasible for the monitoring of tetrachlorvinphos in environmental samples.

3.10. Determination of tetrachlorvinphos in ground and waste water samples

The feasibility of m-AgSAE for the determination of tetrachlorvinphos in the ground and waste water samples is demonstrated in Fig. 10A and B. The SWV analysis under optimized experimental condition did not show the signal for tetrachlorvinphos, and subsequently, the standard addition method was adopted for the recovery studies. The results for different concentrations of tetrachlorvinphos detected by SWV are summarized in Table 4. The recovery was in the range of 93.1–106.2% with RSD below 3%, implying that the proposed method was capable of practical tetrachlorvinphos detection.

Table 4 Measurement results of tetrachlorvinphos in the ground and waste water samples.

Sample	Added (µM)	Found (µM)	Recovery (%)	RSD (%)
Ground water	10	10.62	106.2	1.1
	30	30.90	103.5	1.0
	50	50.55	101.1	0.5
Waste water	10	9.88	98.8	1.5
	30	29.16	97.2	1.5
	50	46.55	93.1	2.6

4. Conclusion

A mercury meniscus modified solid silver amalgam electrode based sensitive, fast, and direct electrochemical sensing platform for organophosphate pesticide tetrachlorvinphos is demonstrated. Taking advantage of its promising characteristics, the m-AgSAE exhibited strong DPV and SWV signals in pH 7 acetate buffer for the reduction of tetrachlorvinphos. The reduction of tetrachlorvinphos is not completely diffusion controlled as reported for its analogs, in fact, it is a diffusion

Please cite this article in press as: N. Al-Qasmi et al., Mercury meniscus on solid silver amalgam electrode as a sensitive electrochemical sensor for tetrachlorvinphos, Journal of Saudi Chemical Society (2016), http://dx.doi.org/10.1016/j.jscs.2016.07.005

controlled adsorption process on m-AgSAE. It has been reported that the voltammetric signals for tetrachlorvinphos may not be very strong in pH 7 buffer solution due to non-availability of protons, however, since we found maximum peak current in pH 7 acetate buffer for tetrachlorvinphos, the analytical application of the proposed method in pH 7 buffer solution becomes possible. It is believed that the m-AgSAE with its higher catalytic efficiency, better analytical performance, non-toxicity, and stability in the environment can be combined with portable electrochemical instrument for the monitoring of tetrachlorvinphos and its analogs in the laboratory as well as in the field. The proposed method is thus simple, cost-effective, and free from complicated instrumental setup.

Acknowledgements

The study, supported by the Center of Excellence in Environmental Studies (CEES), King Abdulaziz University, and the Ministry of Higher Education (MOHE).

Appendix A. Supplementary data

Supplementary data associated with this article can be found, in the online version, at http://dx.doi.org/10.1016/j.jscs.2016.07.005.

References

[1] G.A. Mostafa, Electrochemical biosensors for the detection of pesticides, Open Electrochem. J. 2 (2010) 22–42.
[2] M. Stoytcheva, R. Zlatev, Z. Velkova, B. Valdez, Organophosphorus pesticides determination by electrochemical biosensors, in: M. Stoytcheva (Ed.), Strategies for Pesticides Analysis, INTECH, Croatia, 2011, pp. 359–372.
[3] P. Kumar, K.-H. Kim, A. Deep, Recent advancements in sensing techniques based on functional materials for organophosphate pesticides, Biosens. Bioelectron. 70 (2015) 469–481.
[4] D.G. Peters, C.M. McGuire, E.M. Pasciak, A.A. Peverly, L.M. Strawsine, E.R. Wagoner, J.T. Barnes, Electrochemical dehalogenation of organic pollutants, J. Mex. Chem. Soc. 58 (2014) 287–302.
[5] B. Lozowicka, Health risk for children and adults consuming apples with pesticide residue, Sci. Total Environ. 502 (2015) 184–198.
[6] M.F. Lemos, M.F. Lemos, H.P. Pacheco, R. Scherer, Monitoring of organophosphorous pesticide residues in samples of banana, papaya, and bell pepper, Quím. Nova 38 (2015) 268–273.
[7] H.J. Rectenwald, Neurobehavioral Effects of Chronic Low-level Pesticide Exposure in Children, Department of Public Health and Preventive Medicine, Oregon Health & Science University, 2010.
[8] R. Chandra, S. Chaudhary, Persistent organic pollutants in environment and their health hazards, Int. J. Bioassays 2 (2013) 1232–1238.
[9] S. Li, H. Gao, J. Zhang, Y. Li, B. Peng, Z. Zhou, Determination of insecticides in water using in situ halide exchange reaction-assisted ionic liquid dispersive liquid–liquid microextraction followed by high-performance liquid chromatography, J. Sep. Sci. 34 (2011) 3178–3185.
[10] O.P. Luzardo, M. Almeida-González, N. Ruiz-Suárez, M. Zumbado, L.A. Henríquez-Hernández, M.J. Meilán, M. Camacho, L.D. Boada, Validated analytical methodology for the simultaneous determination of a wide range of pesticides in human blood using GC–MS/MS and LC–ESI/MS/MS and its application in two poisoning cases, Sci. Justice 55 (2015) 307–315.
[11] L. Maggi, M. Carmona, C.P. del Campo, A. Zalacain, J.H. de Mendoza, F.A. Mocholí, G.L. Alonso, Multi-residue contaminants and pollutants analysis in saffron spice by stir bar sorptive extraction and gas chromatography–ion trap tandem mass spectrometry, J. Chromatogr. A 1209 (2008) 55–60.
[12] C. Rasche, B. Fournes, U. Dirks, K. Speer, Multi-residue pesticide analysis (gas chromatography – tandem mass spectrometry detection)–improvement of the QuEChERS (quick, easy, cheap, effective, rugged, and safe) method for dried fruits and fat-rich cereals–benefit and limit of a standardized apple purée calibration, J. Chromatogr. A 1403 (2015) 21–31.
[13] R. Vargas-Bernal, E. Rodríguez-Miranda, G. Herrera-Pérez, Evolution and expectations of enzymatic biosensors for pesticides, in: R.P. Soundararajan (Ed.), Advances in Chemical and Botanical Pesticides, INTECH, Croatia, 2012.
[14] S. de Marcos, E. Callizo, E. Mateos, J. Galbán, An optical sensor for pesticide determination based on the autoindicating optical properties of peroxidase, Talanta 122 (2014) 251–256.
[15] J.S. Van Dyk, B. Pletschke, Review on the use of enzymes for the detection of organochlorine, organophosphate and carbamate pesticides in the environment, Chemosphere 82 (2011) 291–307.
[16] G. Marrazza, Biosensors for organophosphate and carbamate pesticides: a review, Biosensors 4 (2014) 301–317.
[17] M.S. Giri Nandagopal, R. Antony, S. Rangabhashiyam, N. Selvaraju, Advance approach on environmental assessment and monitoring, Res. J. Chem. Environ. 18 (2014) 78–90.
[18] H. Guan, J. Jiang, D. Chen, W. Wang, Y. Wang, J. Xin, Acetylcholinesterase biosensor based on chitosan/ZnO nanocomposites modified electrode for amperometric detection of pesticides, International Conference on Materials, Environmental and Biological Engineering, Atlantis Press, 2015.
[19] G. Anjum, G. Ashish, C. Anil, K.H. Vikas, Electrochemical biosensors for determination of organophosphorus compounds: review, Open J. App. Biosensor 1 (2012) 1–8.
[20] H. Li, J. Li, Z. Yang, Q. Xu, X. Hu, A novel photoelectrochemical sensor for the organophosphorus pesticide dichlofenthion based on nanometer-sized titania coupled with a screen-printed electrode, Anal. Chem. 83 (2011) 5290–5295.
[21] J. Qian, Z. Yang, C. Wang, K. Wang, Q. Liu, D. Jiang, Y. Yan, K. Wang, One-pot synthesis of $BiPO_4$ functionalized reduced graphene oxide with enhanced photoelectrochemical performance for selective and sensitive detection of chlopyrifos, J. Mater. Chem. A 3 (2015) 13671–13678.
[22] C.I.L. Justino, A.C. Freitas, R. Pereira, A.C. Duarte, T.A.P. Rocha, Santos, recent developments in recognition elements for chemical sensors and biosensors, Trends Anal. Chem. 68 (2015) 2–17.
[23] P. Wang, W. Dai, L. Ge, M. Yan, S. Ge, J. Yu, Visible light photoelectrochemical sensor based on Au nanoparticles and molecularly imprinted poly (o-phenylenediamine)-modified TiO_2 nanotubes for specific and sensitive detection chlorpyrifos, Analyst 138 (2013) 939–945.
[24] Ø. Mikkelsen, K.H. Schrøder, Amalgam electrodes for electroanalysis, Electroanalysis 15 (2003) 679–687.
[25] B. Yosypchuk, J. Barek, Analytical applications of solid and paste amalgam electrodes, Crit. Rev. Anal. Chem. 39 (2009) 189–203.
[26] J. Barek, J. Fischer, T. Navrátil, K. Pecková, B. Yosypchuk, J. Zima, Nontraditional electrode materials in environmental

analysis of biologically active organic compounds, Electroanalysis 19 (2007) 2003–2014.
[27] A. Danhel, J. Barek, Amalgam electrodes in organic electrochemistry, Curr. Org. Chem. 15 (2011) 2957–2969.
[28] J. Barek, J. Fischer, J.C. Moreira, J. Wang, Voltammetric and amperometric determination of biologically active organic compounds using various types of silver amalgam electrodes, Sens. Electroanal. 8 (2014) 35–47.
[29] L. Bandžuchová, R. Šelešovská, Voltammetric determination of folic Acid using liquid mercury free silver amalgam electrode, Acta Chim. Slov. 58 (2011) 776–784.
[30] A.M.J. Barbosa, T.A. de Araujo, M.A.G. Trindade, V.S. Ferreira, Direct cefepime determination in human milk using solid mercury amalgam electrode manufactured with silver nanoparticles, J. Electroanal. Chem. 681 (2012) 127–132.
[31] J. Fischer, L. Vanourkova, A. Danhel, V. Vyskocil, K. Cizek, J. Barek, K. Peckova, B. Yosypchuk, T. Navratil, Voltammetric determination of nitrophenols at a silver solid amalgam electrode, Int. J. Electrochem. Sci. 2 (2007) 226–234.
[32] M. Jovi'c, D. Manojlovi'c, D. Stankovi'c, A. Mili'c, M. Senti'c, G. Rogli'c, Voltammetric behavior of tembotrione using silver/amalgam electrode, Am. J. Anal. Chem. 4 (2013) 44–50.
[33] M. Jovic, D. Manojlovic, D. Stanković, A. Milić, M. Sentić, G. Roglić, Voltammetric behavior of mesotrione using silver/amalgam electrode, Int. J. Environ. Res. 7 (2013) 165–172.
[34] M. Brycht, S. Skrzypek, J. Robak, V. Guzsvány, O. Vajdle, J. Zbiljić, A. Nosal-Wiercińska, D. Guziejewski, G. Andrijewski, Ultra trace level determination of fenoxanil by highly sensitive square wave adsorptive stripping voltammetry in real samples with a renewable silver amalgam film electrode, J. Electroanal. Chem. 738 (2015) 69–76.
[35] L. Janíková-Bandžuchová, R. Šelešovská, J. Chýlková, V. Nesnídalová, Voltammetric analysis of herbicide picloram on the silver solid amalgam electrode, Anal. Lett. (2015), http://dx.doi.org/10.1080/00032719.2014.979294 (Available Online).
[36] M. Putek, V. Guzsvány, B. Tasić, J. Zarębski, A. Bobrowski, Renewable silver-amalgam film electrode for rapid square-wave voltammetric determination of thiamethoxam insecticide in selected samples, Electroanalysis 24 (2012) 2258–2266.
[37] K. Nováková, T. Navrátil, J. Dytrtová, J. Chýlková, The use of copper solid amalgam electrodes for determination of the pesticide thiram, J. Solid State Electrochem. 17 (2013) 1517–1528.
[38] H.R. Andersen, F. Debes, C. Wohlfahrt-Veje, K. Murata, P. Grandjean, Occupational pesticide exposure in early pregnancy associated with sex-specific neurobehavioral deficits in the children at school age, Neurotoxicol. Teratol. 47 (2015) 1–9.
[39] B. Senthilkumaran, Pesticide- and sex steroid analogue-induced endocrine disruption differentially targets hypothalamo–hypophyseal–gonadal system during gametogenesis in teleosts – a review, Gen. Comp. Endocrinol. 219 (2015) 136–142.
[40] K.Z. Guyton, D. Loomis, Y. Grosse, F. El Ghissassi, L. Benbrahim-Tallaa, N. Guha, C. Scoccianti, H. Mattock, K. Straif, Carcinogenicity of tetrachlorvinphos, parathion, malathion, diazinon, and glyphosate, Lancet Oncol. 16 (2015) 490–491.
[41] Y. Ni, P. Qiu, S. Kokot, Simultaneous determination of three organophosphorus pesticides by differential pulse stripping voltammetry and chemometrics, Anal. Chim. Acta 516 (2004) 7–17.
[42] D. De Souza, S.S. Machado, Electroanalytical method for determination of the pesticide dichlorvos using gold-disk microelectrodes, Anal. Bioanal. Chem. 382 (2005) 1720–1725.
[43] N. Sreedhar, P.R.K. Reddy, G.S. Reddy, S. Reddy, Differential pulse polarographic determination of dicrotophos, crotoxyphos and chlorfenvinphos in grains and soils, Talanta 44 (1997) 1859–1863.
[44] D. De Souza, L. Mascaro, O. Fatibello-Filho, The effect of composition of solid silver amalgam electrodes on their electrochemical response, J. Solid State Electrochem. 15 (2011) 2023–2029.
[45] R.M. Bashami, A. Hameed, M. Aslam, I.M.I. Ismail, M.T. Soomro, The suitability of ZnO film-coated glassy carbon electrode for the sensitive detection of 4-nitrophenol in aqueous medium, Anal. Method. 7 (2015) 1794–1801.
[46] N. Al-Qasmi, M. Tahir Soomro, I.M.I. Ismail, Ekram Y. Danish, A.A. Al-Ghamdi, An enhanced electrocatalytic oxidation and determination of 2,4-dichlorophenol on multilayer deposited functionalized multi-walled carbon nanotube/Nafion composite film electrode, Arab. J. Chem. (2015), http://dx.doi.org/10.1016/j.arabjc.2015.08.032.
[47] S. Amin, M. Tahir Soomro, N. Memon, A.R. Solangi, Sirajuddin, T. Qureshi, A.R. Behzad, Disposable screen printed graphite electrode for the direct electrochemical determination of ibuprofen in surface water, Environ. Nanotechnol. Monit. Manag. 1–2 (2014) 8–13.
[48] M. Aslam, M. Tahir Soomro, I.M.I. Ismail, N. Salah, M.A. Gondal, A. Hameed, Sunlight mediated removal of chlorophenols over tungsten supported ZnO: electrochemical and photocatalytic studies, J. Environ. Chem. Eng. 3 (2015) 1901–1911.
[49] P. Zuman, V. Kapetanović, M. Aleksić, Recent developments in electroanalytical chemistry of cephalosporins and cefamycins, Anal. Lett. 33 (2000) 2821–2857.
[50] M. Aleksić, M. Ilić, V. Kapetanović, Adsorptive properties of cefpodoxime proxetil as a tool for a new method of its determination in urine, J. Pharm. Biomed. Anal. 36 (2004) 899–903.
[51] D.A. Hall, D.M. Berry, C.J. Schneider, The electrochemistry of cephalosporin C derivatives: part II. Cephalothin, sodium salt, J. Electroanal. Chem. Interfac. Electrochem. 80 (1977) 155–170.
[52] S.A. Greene, Sittig's Handbook of Pesticides and Agricultural Chemicals, William Andrew, 2005.

Please cite this article in press as: N. Al-Qasmi et al., Mercury meniscus on solid silver amalgam electrode as a sensitive electrochemical sensor for tetrachlorvinphos, Journal of Saudi Chemical Society (2016), http://dx.doi.org/10.1016/j.jscs.2016.07.005